




A synthetic peptide derived of the β_2 – β_3 loop of the plant defensin from *Vigna unguiculata* seeds induces *Leishmania amazonensis* apoptosis-like cell death

Géssika Silva Souza¹ · Laís Pessanha de Carvalho² · Edésio José Tenório de Melo² · Flávia Camila Vieira da Silva¹ · Olga Lima Tavares Machado³ · Valdirene Moreira Gomes¹ · André de Oliveira Carvalho¹ 

Received: 17 June 2019 / Accepted: 10 October 2019 / Published online: 25 October 2019
© Springer-Verlag GmbH Austria, part of Springer Nature 2019

Abstract

For medical use of proteins and peptide-based drugs, it is desirable to have small biologically active sequences because they improve stability, reduce side effects, and production costs. Several plant defensins have their biological activities imparted by a sequence named γ -core. *Vu-Def*, a *Vigna unguiculata* defensin, has activity against *Leishmania amazonensis*, which is one etiological agent of leishmaniasis and for which new drugs are needed. Our intention was to understand if the region comprising the *Vu-Def* γ -core is responsible for the biological activity against *L. amazonensis* and to unveil its mechanism of action. Different microbiological assays with *L. amazonensis* in the presence of the synthetic peptide $A_{36,42,44}\gamma_{32-46}$ *Vu-Def* were done, as well as ultrastructural and fluorescent analyses. $A_{36,42,44}\gamma_{32-46}$ *Vu-Def* showed biological activity similar to *Vu-Def*. $A_{36,42,44}\gamma_{32-46}$ *Vu-Def* (74 μ M) caused 97% inhibition of *L. amazonensis* culture and parasites were unable to regrow in fresh medium. The cells of the treated parasites showed morphological alterations by ultrastructural analysis and fluorescent labelings that corroborate with the data of the organelles alterations. The general significance of our work is based on the description of a small synthetic peptide, $A_{36,42,44}\gamma_{32-46}$ *Vu-Def*, which has activity on *L. amazonensis* and that the interaction between $A_{36,42,44}\gamma_{32-46}$ *Vu-Def*–*L. amazonensis* results in parasite inhibition by the activation of an apoptotic-like cell death pathway.

Keywords Antimicrobial peptide · Cowpea · Parasite · Transmission electron microscopy

Handling Editor: J. Broos.

Electronic supplementary material The online version of this article (<https://doi.org/10.1007/s00726-019-02800-8>) contains supplementary material, which is available to authorized users.

✉ André de Oliveira Carvalho
andre@uenf.br

¹ Laboratório de Fisiologia e Bioquímica de Micro-organismos, Universidade Estadual do Norte Fluminense Darcy Ribeiro, Av. Alberto Lamego, 2000, Parque Califórnia, Campos dos Goytacazes, RJ 28013-602, Brazil

² Laboratório de Biologia Celular e Tecidual, Universidade Estadual do Norte Fluminense Darcy Ribeiro, Campos dos Goytacazes, RJ, Brazil

³ Laboratório de Química e Função de Proteínas e Peptídeos, Universidade Estadual do Norte Fluminense Darcy Ribeiro, Campos dos Goytacazes, RJ, Brazil

Introduction

Plant defensins are basic peptides that have molecular weight between 5 and 6 kDa and have a primary structure composed of 45–54 amino acid residues, arranged in a three-dimensional structure composed of one α -helix and three antiparallel β -sheets stabilized by four disulfide bonds (Fant et al. 1999; Song et al. 2011). These plant peptides have several biological activities (van der Weerden and Marilyn 2013) and among them the antimicrobial activity is striking. Due to several reports showing the increased plant defensins genes expression in response to pathogen infection and reports of transgenic plants expressing them that have become resistant to fungal and insect attacks (Jha and Chattoo 2010; Sarkar et al. 2017), this family of plant peptides is supposed to be involved in plant innate immunity (Carvalho and Gomes 2011; Cools et al. 2017). Based on the aforementioned data, plant defensins constitute the PR-12 group of pathogenesis-related proteins (Sels et al. 2008).

Few plant peptides have been reported to exhibit activity on parasites (McGwire and Kulkarni 2010; Torrent et al. 2012) and amidst them is *Vu-Def*, a defensin from *Vigna unguiculata* (cowpea) seed, which has activity against *Leishmania amazonensis* promastigotes (Souza et al. 2013). It has been described that the biological activity of some representative of the plant defensin peptides is related to an amino acid region located between the β_2 and β_3 strands (Schaaper et al. 2001; Sagaram et al. 2011). This region has also been identified in other defensin family peptides, for example in the Mediterranean mussel MGD₁ (*Mytilus galloprovincialis* defensin one) (Romestand et al. 2003). Later, a work identified a motif encompassing few amino acid residues shared with several peptides with antimicrobial activity belonging to different families, which the authors named γ -core (Yount and Yeaman 2004). The γ -core in plant defensins is located between the β_2 and β_3 strands (Carvalho and Gomes 2011).

In this work, following the idea that the major determinants for the biological activity of some plant defensins is imparted by the amino acid sequence of the γ -core region (de Samblanx et al. 1997; Schaaper et al. 2001) and also by the fact that *Vu-Def* has activity against *L. amazonensis* (Souza et al. 2013), we perform the chemical synthesis of the amino acid region encompassing the β_2 and β_3 strands of *Vu-Def* that comprehend the *Vu-Def* γ -core. Our intention was to understand if this region is responsible for the *Vu-Def*'s biological activity against *L. amazonensis* and to unveil its mechanism of action. Plant defensins have demonstrated low toxicity to different mammal cells at up to 500 $\mu\text{g}/\text{mL}$ including human umbilical vein endothelial cells, human skin-muscle fibroblasts, and red blood cells (Terras et al. 1992). In addition, the *in vivo* prophylactic treatment of murine model of candidiasis (Tavares et al. 2008) along with their wide antimicrobial activity against different microorganisms including bacteria (Pelegrini et al. 2011), fungi (Cools et al. 2017), protozoa (Souza et al. 2013), and even cancer cells (Figueira et al. 2017), altogether suggest that this family of peptides is a promising scaffold for the development of new therapeutic substances (Thevissen et al. 2007). As microorganism, we had chosen the protozoan belonging to the genus *Leishmania* because of the epidemiological importance of this genus (Pace 2014). *Leishmania* is a genus of intracellular flagellated protozoan belonging to the order Kinetoplastida encircling more than 20 different species. They are transmitted to humans by infected female sand flies bites that belonging to the *Phlebotomus* genera in Europe, Africa and Asia and *Lutzomyia* in the Americas. *Leishmania*-infected humans develop leishmaniasis, a disease continuum ranging in severity from self-healing disfiguring skin wounds to lethal visceral manifestation depending on the interaction between the *Leishmania* species and human immune system. The disease is spread in 98 countries of the subtropical and tropical areas of the

world, with an estimated population, residents or travelers, at risk of infection of about 350 million. The disease causes considerable burden on the health system of countries with estimated morbidity of more than 3.7 disability-adjusted life years (Pace, 2014). There are drugs available for the treatment of leishmaniasis such as pentavalent antimonials (sodium stibogluconate and meglumine antimoniate), polyene macrolide (amphotericin B), alkyl phosphocholine compound (miltefosine), and lipid formulation of amphotericin B. However, despite availability, low efficacy, serious side effects including toxicity, long treatment basis, high price and additionally reports of parasites resistance impose treatment limitations. Therefore, the development of new drugs and delivery modes with improved qualities are urgent (Akbari et al. 2017). In addition, the mechanism of inhibition of this protozoan by this peptide is unknown.

In this work, we describe a small synthetic peptide, called A_{36,42,44}Y₃₂₋₄₆ *Vu-Def*, which has activity on *L. amazonensis* and that the interaction between A_{36,42,44}Y₃₂₋₄₆ *Vu-Def*-*L. amazonensis* results in parasite inhibition by the activation of an apoptotic-like cell death pathway.

Materials and methods

Cell cultures

Promastigote cells of the *Leishmania amazonensis* strain LV 79 were maintained in 5-mL Warren's medium (90% Brain heart broth, Fluka, enriched with 10% heat-inactivated fetal bovine serum (FBS, Gibco), 0.4% hemin (Sigma-Aldrich) and 0.01% folic acid (Sigma-Aldrich)) or RPMI-1640 medium (Sigma-Aldrich) supplemented with 10% FBS at 28 °C for 3 days and a new culture was established every 3 days. The *L. amazonensis* LV 79 cells were provided by Laboratório de Biologia Celular e Tecidual, Centro de Biotecnologias e Biotecnologia, Universidade Estadual do Norte Fluminense Darcy Ribeiro, Campos dos Goytacazes, Rio de Janeiro, Brazil.

*Vu-Def*r obtainment

The recombinant *Vigna unguiculata* (L. Walp.) defensin (*Vu-Def*r) was obtained as previously described by Souza et al. (2013). In brief, the *Vu-Def*r coding sequence was linked into the pET-32 EK/LIC expression vector and the construction cloned into *E. coli* expression strain Rosetta-gami2 (DE3) pLysS according to the instruction manual (Novagen TB055). For *Vu-Def*r induction, a single colony of transformed Rosetta-gami2 (DE3) pLysS was inoculated in TB medium supplemented with ampicillin (50 $\mu\text{g}/\text{mL}$) (Sigma-Aldrich) and chloramphenicol (34 $\mu\text{g}/\text{mL}$) (Sigma-Aldrich) and incubated at 37 °C for 16 h at 250 rpm. After

this period, 1 mL of that culture was inoculated at 50 mL of fresh supplemented TB medium and incubated as aforementioned until the optical density at 600 nm reaches 0.5–1.0. Then, 1 mM of IPTG was added and the incubation conditions were changed to 30 °C for 3 h at 250 rpm. Cells were recovered by centrifugation at 15,400 \times g for 10 min at 4 °C, resuspended in resuspension buffer (50 mM sodium phosphate, pH 8.0, 300 mM NaCl) containing protease inhibitor cocktail (protease inhibitor cocktail for general use, Sigma-Aldrich) and lysed by the CellLytic B Cell Lysis Reagent according to the instruction manual (Sigma-Aldrich). An aliquot of the supernatant consisting of 30 mg of protein was applied to a Ni⁺-NTA agarose column (Qiagen) which was previously equilibrated in resuspension buffer and the run was developed as described in the column instruction manual (QIAexpressionist, Qiagen). The purified *Vu*-Defr fused with the thioredoxin and six consecutive His was cleavage with enterokinase according to the protease instruction manual (Sigma-Aldrich). After cleavage, the *Vu*-Defr final purification was accomplished in a C18 reversed-phase column (Shim-pack VP-ODS 250L \times 4.6, Shimadzu) attached to a C8 pre-column (20 \times 4.6 mm, Pelliguard, Sigma-Aldrich) in an HPLC (Prominence, Shimadzu) according to Souza et al. (2013).

Vu-Defr modeling

The structural model of *Vu*-Defr was modeled using the Modeller program (Šali and Blundell 1993). For this, it was necessary to have a template (a protein with known three-dimensional structure) to predict the target protein structural model and the sequence obtained in the protein sequence database (Blastp) (Altschul et al. 1990) with the highest similarity with *Vu*-Defr was used. After obtaining the structural model of *Vu*-Defr, its stereochemical quality was checked through the Procheck program and Profile 3D, available on the PARMODEL web server (Laskowski 1993; Uchôa et al. 2004).

Synthetic peptide

Based on the literature information on the γ -core of defensins (Schaaper et al. 2001; Yount and Yeaman, 2004; Sagaram et al. 2011) and on the *Vu*-Defr structural model (as determined in “*Vu*-Defr Modeling”), an amino acid stretch from the loop region between two β -strands (β_2 and β_3) and also part of the intervenient β_2 and β_3 strands of the *Vu*-Defr was selected to be synthesized. The synthesized peptide comprised a stretch of 15 amino acid residues and the three cysteine residues were replaced by L-alanine residues. The synthetic peptide sequence was L₃₂SGRARDDVRAWATR₄₆. The peptide was acquired commercially by AminoTech (Rio de Janeiro, Brazil). The synthetic peptide was dissolved

in pure water to the concentration of 1.1 M. The molecular weight and isoelectric point of the synthetic peptide were determined by Expasy Compute pI/Mw tool (Bjellqvist et al. 1993, 1994; Gasteiger et al. 2005).

Analysis of the biological activity of the synthetic peptide on *L. amazonensis* promastigotes by culture growth inhibition assay

In our previous work (Souza et al. 2013), we established that *Vu*-Defr at concentration of 100 μ g/mL, correspondent to 18.5 μ M, and incubation time of 24 h at 28 °C caused the inhibition of 54.3% of *L. amazonensis* from culture. Therefore, we chose this initial concentration and time as a comparison parameter for the toxicity assays for the synthetic peptide. For culture growth inhibition assay, initially the synthetic peptide and *Vu*-Defr, that were previously resuspended in water, were diluted to 18.5 μ M in supplemented RPMI-1640 medium containing 1.5% dimethyl sulfoxide (DMSO, Sigma-Aldrich) and sterilized by filtration (Millex-GV 0.22 μ m, Millipore). For parasites, an aliquot of the *L. amazonensis* promastigotes cell culture was counted in a Neubauer chamber (LaborOptik). For the assay, control consisted of 4.5 μ L of DMSO (1.5% at final volume of the assay) with 295.5 μ L of supplemented RPMI-1640 medium with parasites. Treated samples consisted of 4.5 μ L of DMSO, peptides at the concentration of 18.5 μ M with supplemented RPMI-1640 medium at maximum volume of 150 μ L and 150 μ L of supplemented RPMI-1640 medium with parasites. The final assay volume was 300 μ L, the initial cell number was 1.5×10^6 promastigotes/mL and it was incubated at 28 °C for 24 h. The number of parasite was counted in a Neubauer chamber after 24 h of incubation.

The growth inhibition assay with the synthetic peptide at concentrations of 18.5 and 74 μ M was done as described above, and the parasite cell number was counted after 24 and 48 h of incubation. This assay, and all subsequent ones, was done with the supplemented Warren's medium.

The growth inhibition assay with the synthetic peptide at concentration of 74 μ M was done as described above, and the parasite cell number was counted at 0, 4, 8, 16, 24, 32 and 48 h of incubation.

Growth recovery assay

After 48 h of incubation with the synthetic peptide at 74 μ M as described in “Analysis of the biological activity of the synthetic peptide on *L. amazonensis* promastigotes by culture growth inhibition assay”, with the exception this repetition was done with supplemented Warren's medium, the cells of *L. amazonensis* were harvested by centrifugation (10 min, 500 \times g, 21 °C). Next, these cells were washed in Warren's medium and incubated with new Warren's medium

at 28 °C for 24 h in the absence of the synthetic peptide. The number of parasite was determined as described in “[Analysis of the biological activity of the synthetic peptide on *L. amazonensis* promastigotes by culture growth inhibition assay](#)”.

Synchronization of *L. amazonensis* cells by 1 mM hydroxyurea

Hydroxyurea (HU) was selected to synchronize the culture because it is a known substance with this effect on cells. HU halt the cell cycle at the G1/S phase. The cell cycle progresses to S phase after cell washing with fresh medium to remove HU (Ashibara and Baserga 1979). For this assay, the HU concentration necessary for cell cycle synchronization was initially determined. For this, an aliquot of the cell culture had its cell number adjusted to 1.5×10^6 promastigotes/mL. Then, the cell culture was incubated with HU at 0.5, 1.0 and 2.0 mM for 12 h. The HU was diluted in supplemented Warren’s medium and sterilized by filtration (Millex-GV 0.22 µm, Millipore). Next, the HU-treated cells were washed by centrifugation (10 min, 500×g, 21 °C) and incubated with fresh supplemented Warren’s medium at 28 °C for 48 h. The number of parasite was counted in a Neubauer chamber at 24 and 48 h. Control consisted of supplemented Warren’s medium with parasites. The final assay volume was 300 µL. The culture was considered synchronized at the HU concentration that halts the cell number increasing determined by the cell counting.

After determining the HU concentration required for cell synchronization as described above, the assay was repeated at the chosen HU concentration (1 mM) with the following modifications: the HU-treated culture after washing was incubated with 74 µM of synthetic peptide for 48 h. The number of parasite cells was counted in a Neubauer chamber at 0, 8, 24 and 48 h.

Ultrastructural analysis of *Leishmania amazonensis* promastigote in the presence of synthetic peptide

The cell culture of *L. amazonensis* promastigotes was treated as described in “[Analysis of the biological activity of the synthetic peptide on *L. amazonensis* promastigotes by culture growth inhibition assay](#)” with the following modification: this repetition was done with supplemented Warren’s medium, incubation time of 8 h at 28 °C in the absence (control) and presence (treated) of 74 µM of the synthetic peptide. After incubation, cells were prepared as described by Carvalho et al. (2010) and Carvalho and Melo (2018). In brief, after the treatments, the samples were washed in phosphate-buffered saline pH 7.2 at 37 °C and fixed at room temperature with Karnovsky’s solution (1% (V/V) glutaraldehyde, 4% (V/V) paraformaldehyde, 5 mM CaCl₂, 5% (W/V) sucrose, and 100 mM cacodylate

buffer, pH 7.2), and then post-fixed for 1 h at room temperature in a solution composed of 2% (V/V) OsO₄, 0.8% (V/V) potassium ferrocyanide, and 5 mM CaCl₂. After fixations, promastigotes were rinsed with 100 mM cacodylate buffer pH 7.2, dehydrated in graded acetone, and embedded in PolyBed812 (Fluka). After, the resin was polymerized for 2 days in 60 °C. Ultra-thin sections obtained with an ultramicrotome (LEICA) were stained with uranyl acetate and lead citrate, and observed with a JEOL 1400Plus Transmission Electron Microscope (TEM) at 60 kV acceleration.

Analysis of the nuclear integrity of *L. amazonensis* cells treated with synthetic peptide by ethidium bromide dye

The cell culture of *L. amazonensis* promastigotes was treated as described in “[Analysis of the biological activity of the synthetic peptide on *L. amazonensis* promastigotes by culture growth inhibition assay](#)” with the following differences: this repetition was done with supplemented Warren’s medium, incubated for 8 h at 28 °C in the absence (control) and presence (treated) of 74 µM of the synthetic peptide. After incubation, the cells were treated with 100 µM of ethidium bromide dye for 20 min. This dye intercalates double-stranded DNA and RNA and became intensely fluorescent. The cells were observed on the Axioplan optical microscope (Zeiss) coupled with a DP72 digital camera (Olympus) using detection filters (excitation: 546 nm; emission: 600 nm) (Baskić et al. 2006).

Analysis of the mitochondria membrane potential in *L. amazonensis* cells treated with synthetic peptide using rhodamine 123 dye

The cell culture of *L. amazonensis* promastigotes was treated as described in “[Analysis of the biological activity of the synthetic peptide on *L. amazonensis* promastigotes by culture growth inhibition assay](#)” with the following differences: this repetition was done with supplemented Warren’s medium, and *L. amazonensis* promastigotes were incubated for 4 h at 28 °C in the absence (control) and presence (treated) of 74 µM of the synthetic peptide. To observe if the synthetic peptide caused some effect on the mitochondrial membrane potential after the incubation time, rhodamine 123 dye was added to the assay at 20 µM as described in rhodamine 123 instruction manual (Thermo Fisher). For this assay, the cells were observed on the Axioplan optical microscope (Zeiss) coupled with a DP72 digital camera (Olympus) using detection filters (excitation: 503 nm; emission: 527 nm).

Analysis of vesicular acidification of *L. amazonensis* cells treated with synthetic peptide by acridine orange dye

The cell culture of *L. amazonensis* promastigotes was treated as described in “Analysis of the biological activity of the synthetic peptide on *L. amazonensis* promastigotes by culture growth inhibition assay” with the following differences: this repetition was done with supplemented Warren’s medium, and *L. amazonensis* promastigotes were incubated for 4 h at 28 °C in the absence (control) and presence (treated) of 74 μ M of synthetic peptide. After the treatment, the cells were incubated with a solution of acridine orange at 5 μ g/mL (Sigma-Aldrich) for 20 min in the absence of light. Acridine orange is a cell-permeant nucleic acid binding dye that emits green fluorescence when bound to double-stranded DNA (excitation: 502 nm; emission: 525 nm) and red fluorescence when bound to single-stranded DNA or RNA (excitation: 460 nm; emission: 650 nm). This dye also enters acidic compartments such as lysosomes, where it becomes protonated and sequestered, and in low pH, acridine orange emits orange fluorescence (emission: 590 nm) when excited by blue light (475 nm) (Cayman chemical manual). For this assay, the cells were observed on the Axioplan optical microscope (Zeiss) coupled with a DP72 digital camera (Olympus) using appropriate detection filters (Carvalho et al. 2010).

Effects of temperature on the bioactivity of the synthetic peptide on *L. amazonensis* promastigotes

The assay was done as described in “Analysis of the biological activity of the synthetic peptide on *L. amazonensis* promastigotes by culture growth inhibition assay” with the following differences: this repetition was done with supplemented Warren’s medium, the cell culture was incubated the synthetic peptide at concentration of 74 μ M for 4 h at 4 °C and after the first 4 h at 4 °C, the cell culture was incubated for another 4 h at 28 °C.

Statistical analysis

Each assay was done three times and in triplicate. Statistical analyses were performed by Tukey’s or Sidak tests using Prism software (version 5.0).

Results and discussion

To synthesize a peptide containing the *Vu*-Def γ -core, first we obtained the *Vu*-Defr structural model based on the *VrD*₂ (*Vigna radiata* defensin two) (PDB ID: 2GL1)

three-dimensional structure as protein model. *VrD*₂ is 91.6% similar to *Vu*-Defr, differing in only four positions (green amino acids in Fig. 1a), and by the first amino acid residue, a methionine (red amino acid in Fig. 1a). This methionine was added to the *Vu*-Defr sequence as a requirement for cloning it into the pET-32 EK/LIC vector (Santos et al. 2010). The Ramachandran plot values of the *Vu*-Defr structural model are shown in Supplementary Fig. 1. The structural model of *Vu*-Defr consists of one α -helix and three antiparallel β -sheets (Fig. 1b) as reported for other plant defensins (Fant et al. 1999) and, in addition, as previously demonstrated by Santos et al. (2010), the addition of the Met₁ did not interfere in the structural model of *Vu*-Defr. Based on the structural model of *Vu*-Defr, we were able to select the amino acid residues that encompass the γ -core (highlighted in blue in Fig. 1a), part of the β_2 strand (Lys₃₂ and Ser₃₃), and part of the β_3 strand (Trp₄₃, Cys₄₄, Thr₄₅ and Arg₄₆) (Fig. 1a). The three cysteine residues were replaced by alanine in the selected sequence, yielding the peptide L₃₂SGRARDDVRAWATR₄₆ (Fig. 1c) which was commercially acquired. This synthetic peptide was called A_{36,42,44}Y₃₂₋₄₆*Vu*-Def and its chemical characteristics are shown in Fig. 1d. The position of the A_{36,42,44}Y₃₂₋₄₆*Vu*-Def in consideration of to the *Vu*-Def structural model is shown in Fig. 1e which shows only the position of A_{36,42,44}Y₃₂₋₄₆*Vu*-Def in the *Vu*-Def structural model and not its conformation. A_{36,42,44}Y₃₂₋₄₆*Vu*-Def had their cysteine residues exchanged by alanine residues to prevent the formation of non-existent disulfide bonds in the natural peptide and also to avoid the peptide from having free cysteine residues. The other authors, to solve this same problem, substituted the cysteine residues for the non-protein amino acid α -aminobutyric acid (Schaaper et al. 2001). We exchange cysteine for alanine because alanine is a nonpolar amino acid (has hydrophobic characteristic and is neutral in charge) and has a small volume and non-reactive side chain. Therefore, this substitution cancels side-chain interactions without altering main-chain conformation or including steric or electrostatic effects. In our synthetic peptide, the *Vu*-Def γ -core, as defined by Yount and Yeaman (2004), comprises the amino acid residues G₃₄RCRDDVRC₄₂, but the entire sequence of our synthetic peptide is longer, i.e., L₃₂SGRARDDVRAWATR₄₆ (shown with the Cys substituted by Ala). We chose a longer sequence because the other authors have shown the importance of synthesizing peptides larger than the γ -core itself to improve their antifungal activity (Schaaper et al. 2001; Sagaram et al. 2011). Schaaper et al. (2001) has demonstrated by synthesizing various peptides of different sizes, ranging from 13 to 20 amino acid residues, based on the primary structure of *R*s-AFP₂ (*Raphanus sativus* antifungal peptide two) that the size of the peptide influences its antifungal activity; decreasing the size of the peptide also decreased its antifungal activity and

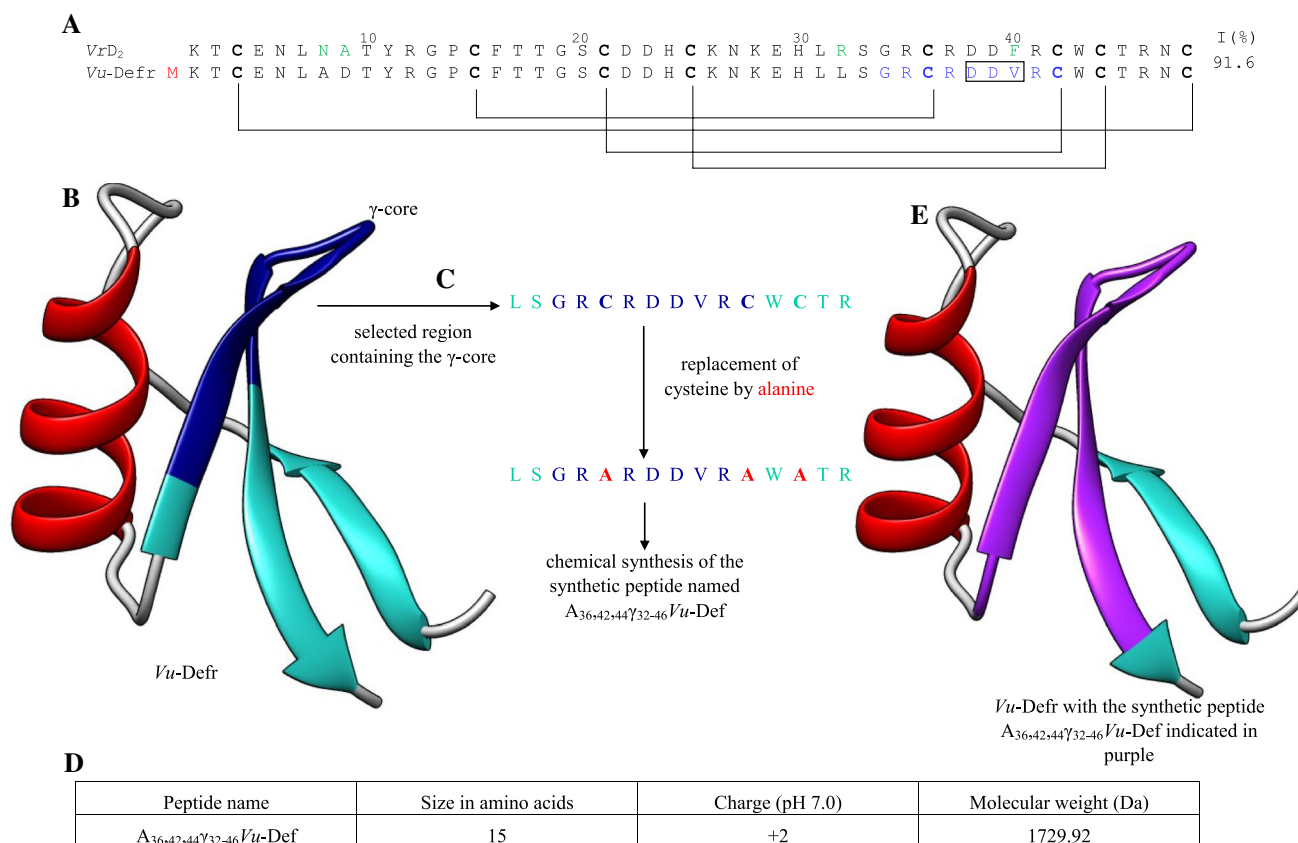


Fig. 1 **a** Alignment of the *Vu-Defr* and *Vigna radiata* defensin 2 (VrD_2) (PDB ID: 2GL1) primary structures. The lines below the Cys residues (highlighted in bold) in *Vu-Defr* indicate the arrangement of disulfide bonds. The four amino acid residues that differ between the two primary structures are marked in green in the VrD_2 sequence. One additional methionine residue was included in the primary structure of *Vu-Defr* as a cloning requirement is marked in red. The amino acid residues marked in dark blue in *Vu-Defr* correspond to the γ -core region as determined by Yount and Yeaman (2004). The amino acid residues marked in a box correspond to a loop region of *Vu-Defr*. The

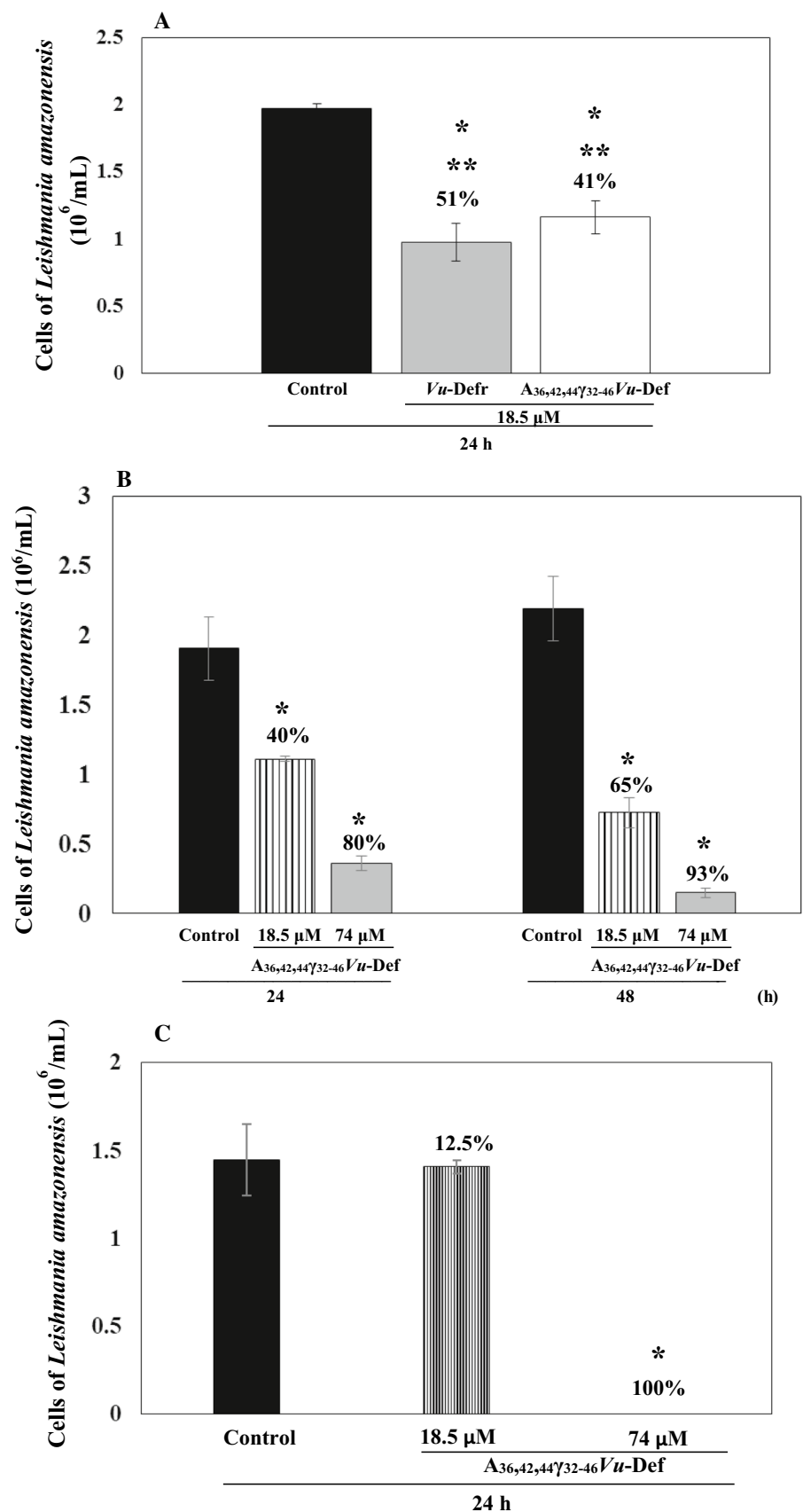
numbers above the sequence indicate the peptide sizes in amino acids according to *Vu-Defr*. I, indicates the percentage of identical amino acids residues between the two peptides. **b** Structural model of *Vu-Defr* modeled with Modeller, based on the three-dimensional structure of VrD_2 . Gray represents unstructured elements, red represents α -helices, light blue represents β sheets, and dark blue represents the γ -core region. **c** Steps of the synthetic peptide design. **d** Chemical properties of the synthetic peptide $A_{36:42;44}Y_{32-46}Vu-Def$. **e** The same as in **b** with the synthetic peptide $A_{36:42;44}Y_{32-46}Vu-Def$ indicated in purple

the highest activity was found in peptides encompassing the whole β_2 and β_3 strands and its connecting loop, where the γ -core is inserted. After designing the experiment, microbiological assays were done to confirm the biological activity of $A_{36:42;44}Y_{32-46}Vu-Def$ against *Leishmania amazonensis* promastigotes.

The $A_{36:42;44}Y_{32-46}Vu-Def$ activity was initially checked by comparing it with the *Vu-Defr* activity in a culture growth inhibition assay against *L. amazonensis* with both peptides at 18.5 μ M and 24 h of incubation (Fig. 2a). The $A_{36:42;44}Y_{32-46}Vu-Def$ was capable of inhibiting 41% of the culture growth compared to the control and *Vu-Defr* was able to inhibit 51%. Despite this difference, it was not statistically significant. Therefore, $A_{36:42;44}Y_{32-46}Vu-Def$ retains biological activity of *Vu-Defr* (Souza et al. 2018). In our previous work (Souza et al. 2013), we established that

Vu-Defr at a concentration of 100 μ g/mL, corresponding to 18.5 μ M, and an incubation time of 24 h caused 54.3% inhibition of *L. amazonensis* culture. For this reason, we have chosen this initial concentration and time as parameters for comparison for synthetic peptide toxicity assays. The strategy of identification and subsequent use of smaller peptides which retain the biological activity of the entire peptide has some advantages to the medical and pharmaceutical areas. First, the identification of the peptide itself unravels a small structure that retains full biological activity. Second, shorter biologically active sequence enable pharmaceutical and medical uses because of lower cost on chemical synthesis and the lower likelihood of immune reaction compared to the whole peptides (Seo et al. 2012). The in vitro biological activity of the $A_{36:42;44}Y_{32-46}Vu-Def$ also point out another good evidence that the $A_{36:42;44}Y_{32-46}Vu-Def$ could

Fig. 2 a Growth of *Leishmania amazonensis* in the absence (control) and in the presence of *Vu*-Defr and of $A_{36,42,44}\gamma_{32-46}$ *Vu*-Def. The percentage of protozoan inhibition is shown above the bars. This result indicates that the synthetic peptide $A_{36,42,44}\gamma_{32-46}$ *Vu*-Def is biologically active. (*) Indicates significance ($p=0.0058$ for *Vu*-Def; $p=0.0106$ for $A_{36,42,44}\gamma_{32-46}$ *Vu*-Def) by the Tukey test ($p<0.05$) among experiments and control. (**) Indicate no significance ($p=0.3394$) by the Tukey test ($p<0.05$) among the *Vu*-Defr and $A_{36,42,44}\gamma_{32-46}$ *Vu*-Def. The graphic was done with the mean and standard deviation of one independent assay. **b** Growth of *L. amazonensis* in the absence (control) and presence of different $A_{36,42,44}\gamma_{32-46}$ *Vu*-Def concentrations. The percentage of protozoan inhibition is shown above the bars. (*) Indicates significance ($p=0.0344$ for 18.5 μ M and 24 h; $p=0.0001$ for 74 μ M and 24 h; $p=0.0013$ for 18.5 and 48 h; $p<0.0001$ for 74 μ M and 48 h) by the Tukey test ($p<0.05$) among the experiments and their respective controls. The graphic was done with the mean and standard deviation of one independent assay. **c** *L. amazonensis* growth recovery assay after culture growth inhibition assay in the presence of $A_{36,42,44}\gamma_{32-46}$ *Vu*-Def. Under the conditions tested, 74 μ M is a lethal concentration for the parasite. The percentage of protozoan inhibition is shown above the bars. (*) Indicates significance ($p<0.0001$) by the Tukey test ($p<0.05$) among the experiments and their respective controls. The graphic was done with the mean and standard deviation of one independent assay



maintain its antimicrobial efficacy in in vivo disease models because its activity is retained in complex media (Warren's and RPMI-1640 media) and also in the presence of serum. This last characteristic reinforces this possibility since other AMPs completely lose their antimicrobial activities in the presence of serum, such as LL-37 (AMP from *Homo sapiens*) (Johansson et al. 1998) and gomesin (AMP from the spider *Acanthoscurria gomesiana*) (Fázio et al. 2006), turning their pharmaceutical uses unfeasible. After confirming the biological activity of the $A_{36,42,44}Y_{32-46}Vu$ -Def, all other experiments were done only with it.

To discover the lethal concentration of $A_{36,42,44}Y_{32-46}Vu$ -Def on *L. amazonensis* promastigotes, a new culture growth inhibition assay was done at concentrations of 18.5 and 74 μ M (Fig. 2b). $A_{36,42,44}Y_{32-46}Vu$ -Def, at concentrations of 18.5 and 74 μ M, inhibited 40 and 80% of *L. amazonensis* culture in 24 h of incubation, respectively, comparing to the control. In addition, after 48 h of incubation $A_{36,42,44}Y_{32-46}Vu$ -Def was able to inhibit 65 and 93%, respectively. This assay was done with supplemented Warren's medium, and despite this medium change, it did not affect the $A_{36,42,44}Y_{32-46}Vu$ -Def activity because the inhibition percentage of $A_{36,42,44}Y_{32-46}Vu$ -Def at 18.5 μ M after 24 h in this medium, i.e., 40%, was practically the same in the RPMI-1640 medium, i.e., 41% (Fig. 2a). The effect of the peptide was tested in RPMI-1640 medium because in future studies, we will test the activity of $A_{36,42,44}Y_{32-46}Vu$ -Def against intracellular amastigotes of *L. amazonensis* that are grown in infected host cells that are cultivated in this medium. All subsequent assays were done with supplemented Warren's medium.

Next, we performed a growth recovery assay to determine whether the remaining parasites in the treated culture were able to recover their viability after $A_{36,42,44}Y_{32-46}Vu$ -Def treatment. We found that $A_{36,42,44}Y_{32-46}Vu$ -Def at the concentration of 18.5 μ M caused 65% of the culture growth inhibition at 48 h (Fig. 2b), the remaining 35% of *L. amazonensis* cells were able to regrow when transferred to a new medium without $A_{36,42,44}Y_{32-46}Vu$ -Def (Fig. 2c). $A_{36,42,44}Y_{32-46}Vu$ -Def at the concentration of 74 μ M caused 93% culture growth inhibition at 48 h (Fig. 2b), the remaining 7% of *L. amazonensis* cells were unable to regrow when transferred to a new medium without $A_{36,42,44}Y_{32-46}Vu$ -Def (Fig. 2c). Therefore, under the conditions tested, 74 μ M is a lethal dose to the parasite. Based on these results, we started working with the most toxic concentrations as determined in our conditions to understand the mechanisms involved in the parasite cell death. The importance of using a lethal concentration of an antimicrobial peptide (AMP) is that there is no misunderstanding on the response signals which lead to the microorganism death with response signals that lead to microorganism recovering as described by Soares et al.

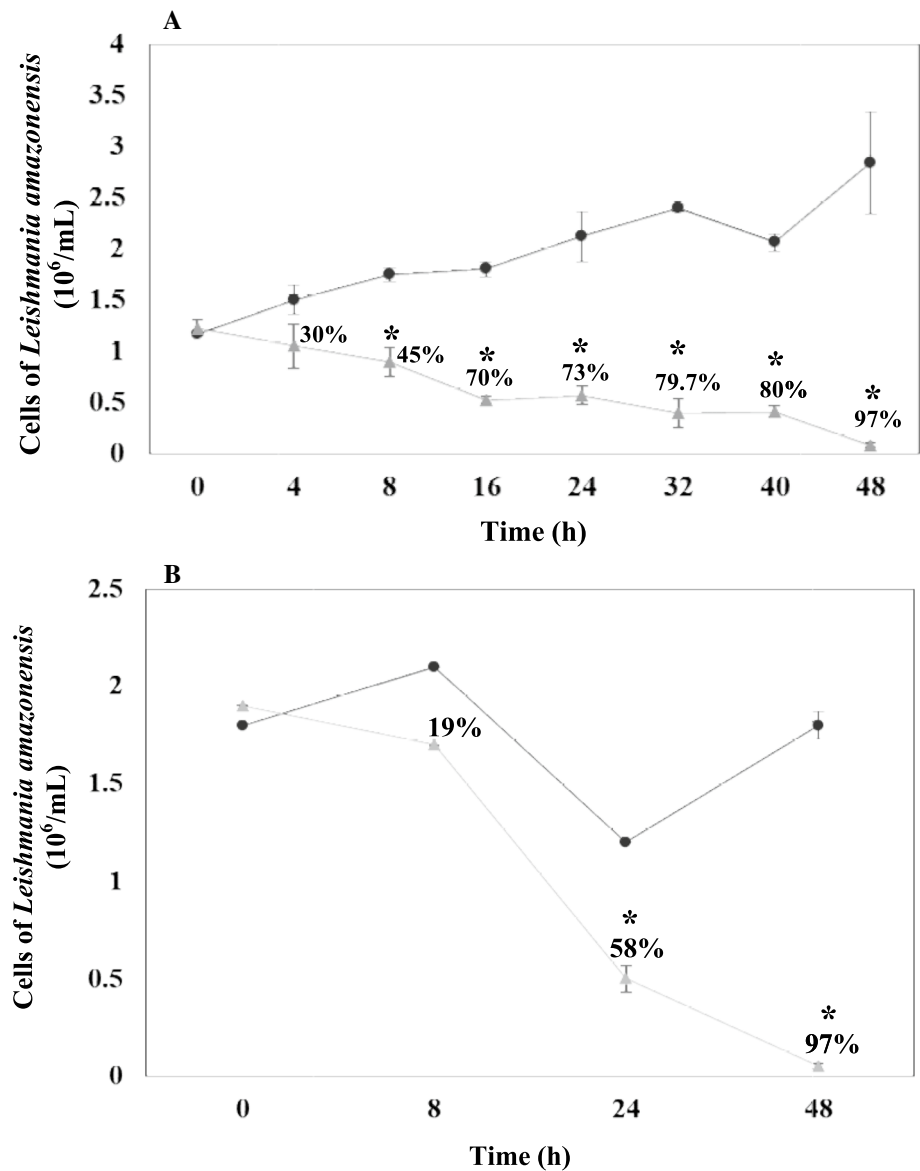
(2017). Those authors worked with the budding yeast *Saccharomyces cerevisiae* and the defensin *ApDef*₁ (*Adenanthera pavonina* defensin one) and suggested that, at lower *ApDef*₁ concentrations, the yeast cells were able to mount a defense response that overcome the pathway leading to induced cell death by *ApDef*₁. Moreover, the use of a lethal concentration of an antimicrobial agent is desirable because it reduces the risk of resistance development by target microorganism (Vieira et al. 2015).

To better understand the growth inhibition process of *L. amazonensis* culture in the presence of 74 μ M of the $A_{36,42,44}Y_{32-46}Vu$ -Def, an assay was carried out in which the culture growth was evaluated at different times (Fig. 3a). The assay indicated that at zero time, no inhibition occurred, but at 4, 8, 16, 32, 40 and 48 h of $A_{36,42,44}Y_{32-46}Vu$ -Def treatment, levels of 30, 45, 70, 73, 79.7, 80 and 97% of parasite inhibition were observed, respectively, compared to the control. By the analysis of the growth culture inhibition at different times (Fig. 3a), we observe that the inhibition of the parasite occurred mostly gradually; at 8–16 h, 1.5–2.3 times greater inhibition of parasites was seen when compared to that at 0–4 h. This higher inhibition index at 8–16 h is coincident to the *L. amazonensis* cell division time, i.e., 8 h, in the condition tested (Result not shown). Taking these results together, we suggest that inhibition of the parasite may be related to some cellular target which is exposed only at a certain stage of the cell cycle.

To verify whether the cell cycle was related or not to the parasite inhibition caused by $A_{36,42,44}Y_{32-46}Vu$ -Def, *L. amazonensis* culture cells were synchronized with 1 mM HU (Fig. 3b). We observe that after 8 h of incubation, the synthetic peptide was able to inhibit 19% of parasites present in the culture as compared to the control. At 24 and 48 h, the peptide inhibited 58 and 97%, respectively. For the unsynchronized culture, the data were: for 8 h, 45.71%, for 24 h, 73% and for 48 h, 97% (see Fig. 3a). Some authors reported that some plant defensins like *PsD*₁ (*Pisum sativum* defensin one) (Lobo et al. 2007) get accesses to the fungal cytoplasm, and, therefore, these defensins are able to interact with intracellular targets. Amidst the intracellular targets that are affected are components of the cell cycle. *PsD*₁ enters in the cytoplasm of the fungus *Neurospora crassa* and binds to cyclin F impairing cell cycle progression (Lobo et al. 2007). Another plant defensin whose mechanism of action was related to the *S. cerevisiae* cell cycle is *ApDef*₁ (Soares et al. 2017). With regard to the involvement of cell cycle in *L. amazonensis* culture growth inhibition, the result of synchronized culture (Fig. 3b) indicates that the peptide action in the first 24 h is 2.3 times less expressive than in the synchronized culture, however, at the time of 48 h, the synchronized protozoan cells are inhibited at the same proportion of the protozoan cells of the unsynchronized culture. This result suggests that *L. amazonensis* inhibition maybe

Fig. 3 a Time course of *Leishmania amazonensis* promastigote growth in the presence of 74 μ M of A_{36:42:44}Y₃₂₋₄₆Vu-Def synthetic peptide. (Dotted circle) corresponds to the protozoan growth and (dotted triangle) corresponds the protozoan inhibition. The percentage of inhibition is shown above the (dotted triangle). (*) Indicates significance ($p=0.0149$ for 8 h; $p=0.0013$ for 16 h; $p=0.0003$ for 24 h; $p<0.0001$ for 32 h; $p=0.003$ for 40 h, and $p<0.001$ for 48 h) by the Sidak's test ($p<0.05$) among the tests and their respective controls.

b Growth of *L. amazonensis* synchronized cell culture in the absence (dotted circle, control) and presence of 74 μ M of the A_{36:42:44}Y₃₂₋₄₆Vu-Def (dotted triangle). The percentage of protozoan inhibition is shown above the (dotted triangle). (*) Indicates significance ($p=0.0198$ for 24 h; $p=0.0006$ for 48 h) by the Tukey's test ($p<0.05$) among the tests and their respective controls. The graphics were done with the mean and standard deviation of one independent assay



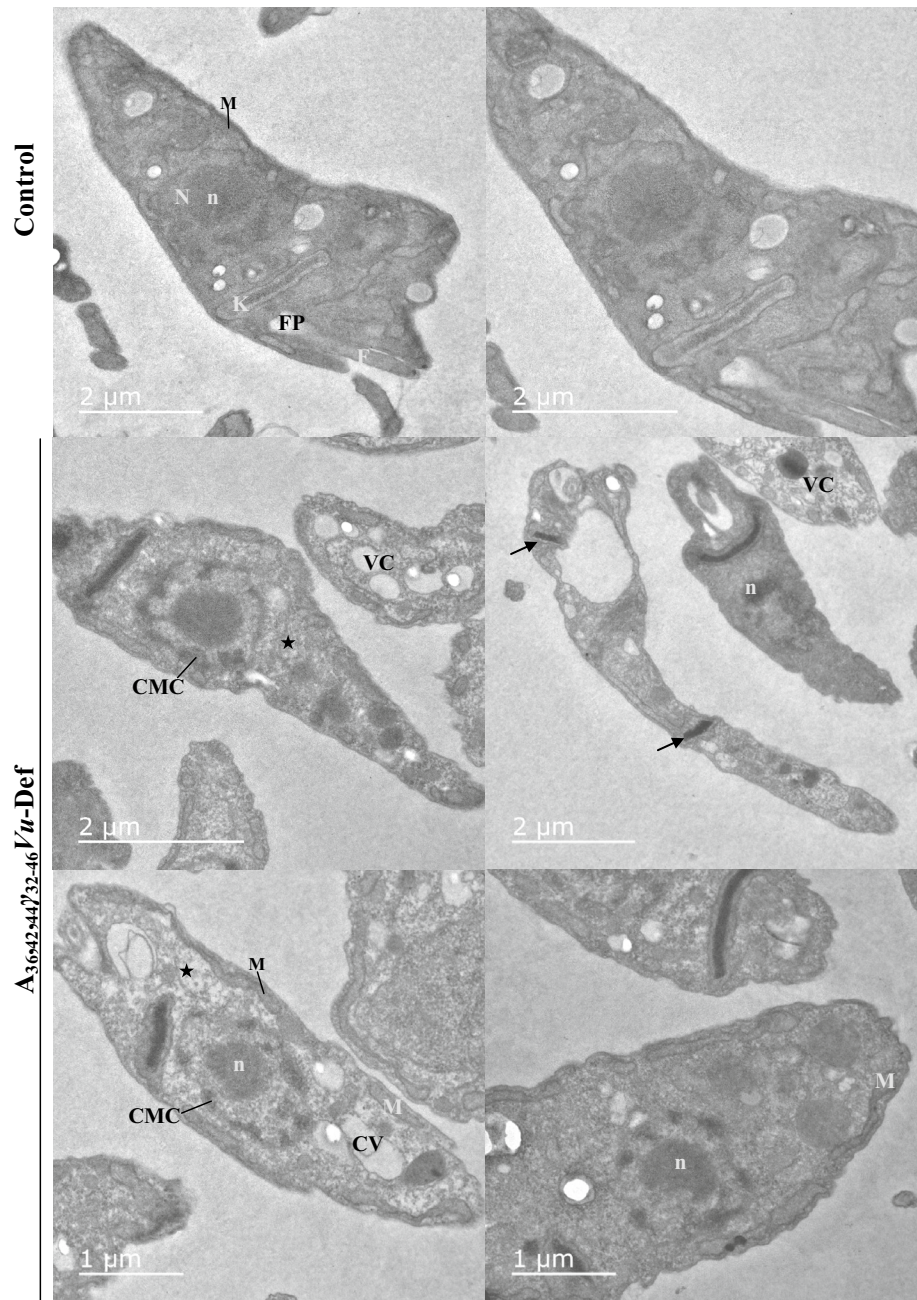
cell cycle dependent, although more studies are needed to unravel the cell cycle involvement.

To understand the toxic effect of A_{36:42:44}Y₃₂₋₄₆Vu-Def on the cell, the analysis of the parasite cellular structures was performed by TEM after 8 h of incubation at 28 °C (Fig. 4). The control cells were slightly slender and present an organized cytoplasm with well-characterized organelles such as nuclei, mitochondria, kinetoplast, and flagellar pocket (Fig. 4). Particularly, the nuclei had a large centrally located nucleolus and chromatin evenly distributed along the nuclear membrane. Treated cells were more rounded, the cytoplasm was granulated, less electron-dense and vacuolated. The plasma membrane appears to be intact. The nuclei present a disorganized chromatin, reduced and distorted nucleolus, and chromatin condensation in the nuclear periphery. Other cell organelles also presented

ultrastructural alterations such as swollen mitochondria and split kinetoplasts which were also more electron-dense (Fig. 4). This ultrastructural analysis of *L. amazonensis* cell by TEM revealed a number of cellular alterations after 8 h of incubation with A_{36:42:44}Y₃₂₋₄₆Vu-Def (Fig. 4). We chose this initial time because we were interested in determining of the first alterations caused in the *L. amazonensis* cells, because the antimicrobial assay had demonstrated that since 4 h A_{36:42:44}Y₃₂₋₄₆Vu-Def causes 30% of promastigote inhibition and at 8 h, it causes 45% of promastigotes inhibition (Fig. 3a). The other authors found similar results after incubation of *Leishmania* species with different compounds (Mangoni et al. 2005; Rodrigues et al. 2014).

After observing the effects caused on the nucleus and kinetoplast of *L. amazonensis* cells by A_{36:42:44}Y₃₂₋₄₆Vu-Def (Fig. 4), after 8 h of incubation, we performed a fluorescence

Fig. 4 Transmission electron microscopy images of *Leishmania amazonensis* promastigote treated with 74 μ M of $A_{36,42,44}\gamma_{32-46}$ *Vu-Def* for 8 h. The treated protozoan cells showed an altered ultrastructural morphology with change in shape which the cells are rounded, the cytoplasm is granulated, less electron-dense and vacuolated. The nuclei presented disorganized chromatin, reduced and distorted nucleolus and chromatin condensation in the nuclear periphery. The mitochondria were swollen and kinetoplast more electron-dense and in some cases, split. The plasma membrane appears to be intact. *N* nucleus, *n* nucleolus, *M* mitochondrion, *K* kinetoplast, *F* flagellum, *FP* flagellar pocket, *CMC* condensed and marginated chromatin, *star* cytoplasm not electron-dense, \rightarrow split kinetoplast, *VC* vacuolated cytoplasm. The images are representative of one independent assay

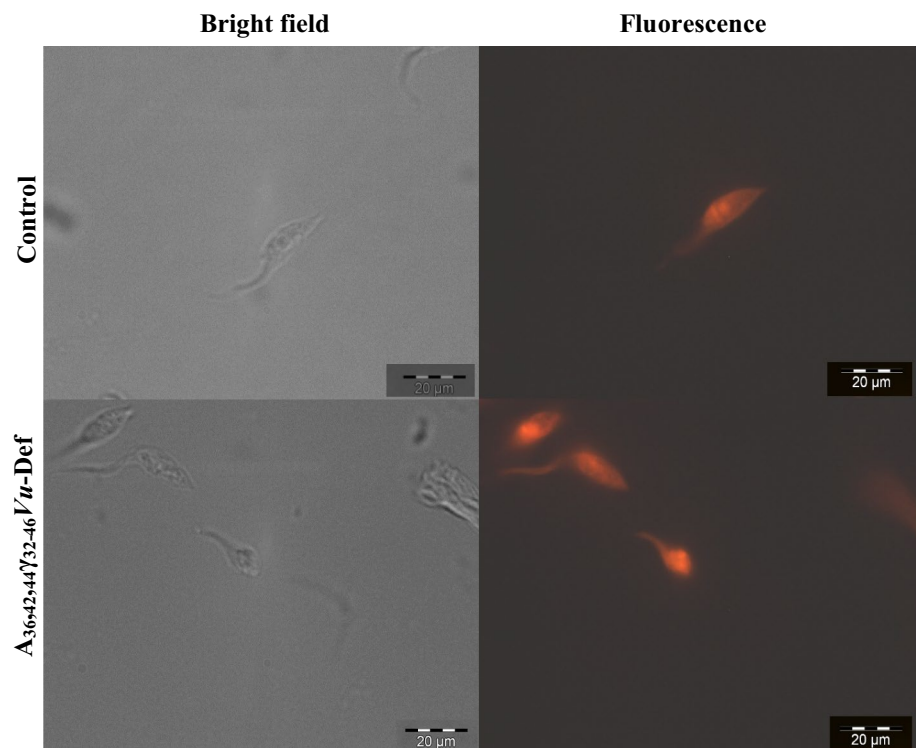


microscopy assay in the presence of ethidium bromide (Fig. 5). The control samples showed a punctual labeling in relation to the nucleus and kinetoplast, which is different from that observed in the treated ones, which presented a diffuse labeling (Fig. 5). Taking together the results of loss of viability (Fig. 2c) and structural alterations in the nuclei (Fig. 4) of the treated cells, it is possible to suggest that an apoptotic cell death pathway might be activated after $A_{36,42,44}\gamma_{32-46}$ *Vu-Def*-*L. amazonensis* interaction. The ethidium bromide-labeling pattern (Fig. 5) suggests DNA fragmentation and nucleus disorganization. The low cell density observed in Fig. 5 is due to the 45% inhibition of

L. amazonensis cell culture caused by its incubation with 74 μ M of the $A_{36,42,44}\gamma_{32-46}$ *Vu-Def* for 8 h (see Fig. 3a). The same phenomenon is observed in Figs. 6 and 7, which also has inhibition as a cause for the low number of cells observed. This result (Fig. 5) corroborates with the results of electron microscopy (Fig. 4) as well as it is one well-characterized feature of apoptosis-induced death (Reece et al. 2011).

Based on the effect that $A_{36,42,44}\gamma_{32-46}$ *Vu-Def* has on mitochondria (Fig. 4), we performed a fluorescence microscopy assay in the presence of rhodamine 123 dye. We could observe that control cells had punctual dye

Fig. 5 Images of *Leishmania amazonensis* promastigotes treated with 74 μ M of $A_{36,42,44}\gamma_{32-46}$ *Vu*-Def for 8 h and incubated with ethidium bromide fluorescent dye. Note the diffuse labeling in the presence of $A_{36,42,44}\gamma_{32-46}$ *Vu*-Def. This labeling pattern suggests DNA fragmentation and nuclear disorganization. Bars = 20 μ m. The images are representative of one independent assay

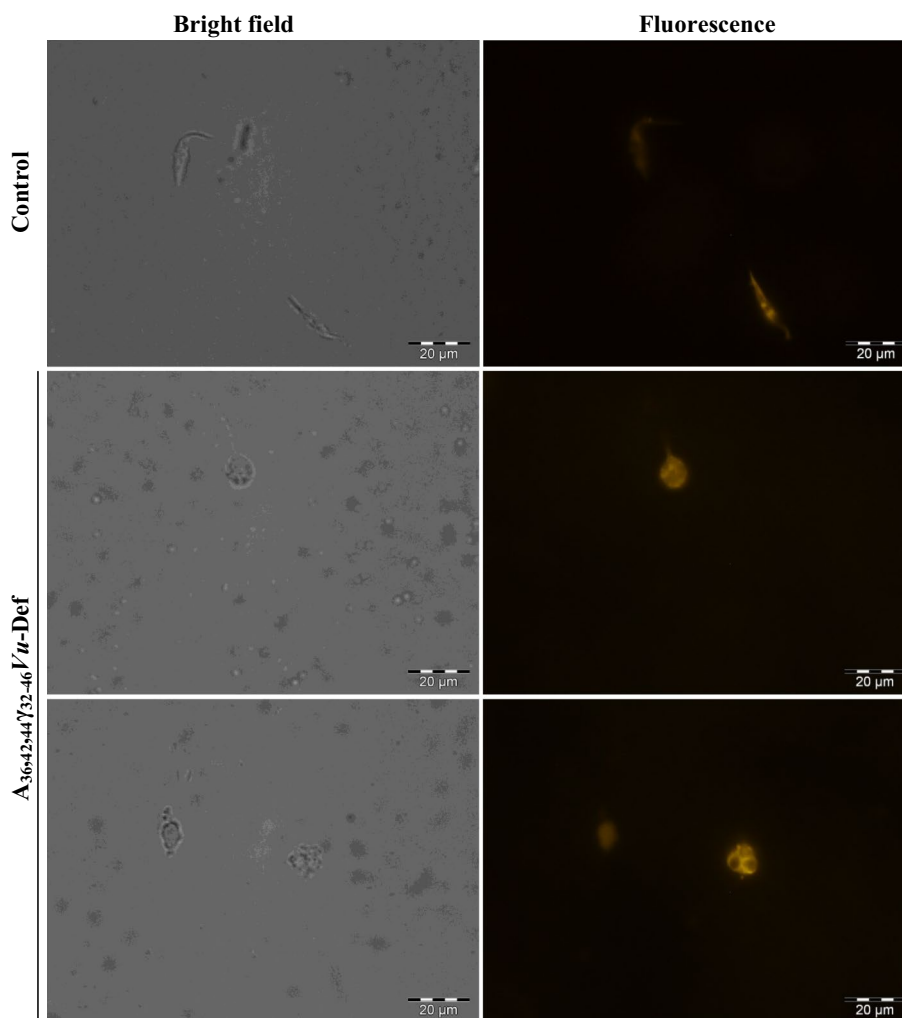


label along the cell cytoplasm (Fig. 6). In the presence of $A_{36,42,44}\gamma_{32-46}$ *Vu*-Def within 4 h of incubation, these punctual labelings were not observed, and instead a diffuse labeling was observed throughout the cell cytoplasm. This diffuse labeling may be related to mitochondrial fragmentation and swelling, and to the vacuolization observed in the TEM images (Fig. 4). The effect of $A_{36,42,44}\gamma_{32-46}$ *Vu*-Def caused in the mitochondria (Figs. 4, 6) indicates that the mitochondria were depolarized and that the membrane potential of other organelles or vesicles may be stimulated due to the higher fluorescence signal observed in the cytoplasm of the treated cells. This interpretation is due to the features of the rhodamine 123 dye that accumulates in places where the electrochemical potential is high. Mitochondrial membrane depolarization has been previously associated with apoptosis cell death in *Leishmania* (Mukherjee et al. 2002), which reinforces our observation of cell death (Fig. 2c) and the morphological features of apoptosis seen by TEM (Fig. 4). Although within 4 h of incubation time, protozoan inhibition was not statistically significant from the control (Fig. 3a), we chose this time point because TEM analysis at 8 h of incubation time indicated great morphological alteration in protozoan cells (Fig. 4) and also because we wanted to discover the first organelles to be affected. This result indicates that in *L. amazonensis* promastigotes treated with $A_{36,42,44}\gamma_{32-46}$ *Vu*-Def, mitochondria are among the first organelles to be affected.

Based on the rhodamine 123 labeling in the cytoplasm which indicated a higher electrochemical potential of

organelles or vesicular membranes, we investigated whether this membrane energization could be due to H^+ fluxes and thus we analyzed their acidification by acridine orange dye. This dye labels acid compartments when excited with blue light (475 nm) and in control samples, the labeling was stronger on nuclei and kinetoplast and in the cytoplasm, the dye labeling was sparse and some regions were not labeled. Instead, in the treated samples, we still observe the nuclei and kinetoplast labelings, but with morphological alterations, and the main alteration occurs in the cytoplasm where the labeling has become diffuse and more intense (Fig. 7, 475 nm). As expected and corroborating the rhodamine 123 labeling analysis (Fig. 6), our result with the acridine orange dye labeling indicates that the cytoplasm and the lumen of some other organelles became acidified already after 4 h incubation with $A_{36,42,44}\gamma_{32-46}$ *Vu*-Def. Similar results were obtained for *L. amazonensis* treated with a fraction of *Bertholletia excelsa* (Brazil nut) where the cytoplasm of treated cells presents a stronger labeling for rhodamine 123 in comparison to the control cells, in which case the labeling indicated that the membrane potential of organelles were altered by the treatment (Fardin et al. 2016). Taking advantage of the capability of acridine orange dye to also emit green fluorescence when bound to double-stranded DNA and excited by green light (502 nm), and since $A_{36,42,44}\gamma_{32-46}$ *Vu*-Def was able to cause morphological alterations in the nuclei (Fig. 4), a fluorescence microscopy assay, after 4 h incubation with $A_{36,42,44}\gamma_{32-46}$ *Vu*-Def, was performed. Figure 7 (502 nm) shows that some treated

Fig. 6 Images of *Leishmania amazonensis* promastigotes treated with 74 μ M of $A_{36^*42,44}\gamma_{32-46}$ *Vu*-Def for 4 h and incubated with the rhodamine 123 fluorescent dye. Note the diffuse labeling in the presence of $A_{36^*42,44}\gamma_{32-46}$ *Vu*-Def. Bars = 20 μ m. The images are representative of one independent assay

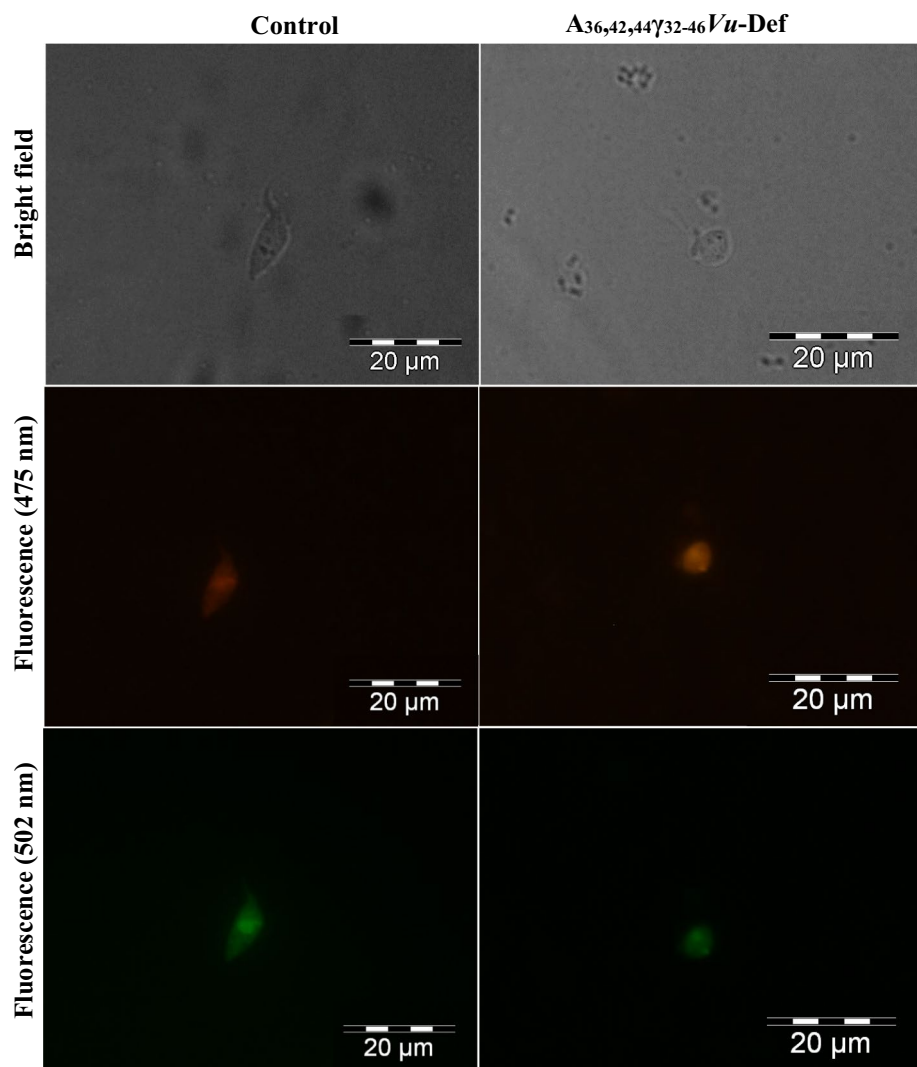


cells had a fragmented labeling than that observed in the control where it is possible to see the labeling of the entire nucleus and kinetoplast. This observation is an indication of chromatin fragmentation, which corroborates the results observed by TEM (Fig. 4) and ethidium bromide dye (Fig. 5). These results show that the cellular morphological alterations had already begun within 4 h of contact with $A_{36^*42,44}\gamma_{32-46}$ *Vu*-Def and are indicative that the nucleus is one of the first organelles to be affected along with mitochondria (Fig. 6). Neto et al. (2011) suggests that the alteration in the green fluorescence of acridine orange observed in *L. chagasi* and *L. amazonensis* treated with *Ocotea duckei* Vattimo lignan occurs due to damage or to conformational changes in nucleic acids.

An assay incubating the parasite for 4 h at 4 °C was performed to understand whether the *L. amazonensis*- $A_{36^*42,44}\gamma_{32-46}$ *Vu*-Def interaction is energy dependent. As can be seen from Fig. 8 that when promastigotes were incubated at 4 °C, $A_{36^*42,44}\gamma_{32-46}$ *Vu*-Def was still able to inhibit 48% of culture growth at 4 h and when the promastigotes were transferred to 28 °C for further 4 h (total incubation time of

8 h), $A_{36^*42,44}\gamma_{32-46}$ *Vu*-Def was capable to inhibit 93% of the parasites culture growth. When the cells are maintained at 28 °C all the time, in the first 4 h of incubation, the peptide was capable of inhibiting 30% growth of the parasites culture and 45% inhibition at 8 h (Fig. 3a). It has already been described that the interaction of some microorganism-AMPs occurs through the electrical potential of microorganism plasma membrane. This was observed for peptides *ApDef*₁ and histatin 5 (an AMP from human saliva) which, when the microorganism was previously treated with carbonyl cyanide 3-chlorophenylhydrazone (CCCP), a membrane depolarizing agent, or the assay was incubated at 4 °C, had their antimicrobial activity inhibited (Soares et al. 2017). Also to *NaD*₁, its entry into *Candida albicans* cells is blocked by CCCP and 4 °C, and the authors concluded that the process by which *NaD*₁ gets access to the yeast cytoplasm is endocytosis (Hayes et al. 2018). Both the depolarizing agent and low temperature decrease cell metabolism and thus inhibit energy-dependent cellular process such as endocytosis. In addition, it was observed that, at 4 °C, the parasite *Trypanosoma cruzi*, belonging to Kinetoplastida order, as well as

Fig. 7 Images of *Leishmania amazonensis* promastigotes treated with 74 μ M of $A_{36,42,44}Y_{32-46}$ *Vu*-Def for 4 h and incubated with the acridine orange fluorescent dye. Our result indicates that cytoplasm and some other organelles lumen became acidified. *K* kinetoplast, *N* nucleus. Bars = 20 μ m. The images are representative of one independent assay



Leishmania spp., had affected the receptor-mediated endocytosis and fluid-phase pinocytosis pathways (de Figueiredo and Soares 2000), preventing the entry of nutrients and even peptides. In view of this, it was expected that at 4 °C, the *L. amazonensis* cells should be protected from the $A_{36,42,44}Y_{32-46}$ *Vu*-Def action. However, our result showed the contrary to expected (Fig. 8) because when the parasites were incubated at 4 °C, the synthetic peptide became more effective in its action, being able to inhibit 93% of the parasites in 8 h. This inhibition rate for the parasite incubated all the time at 28 °C with the peptide is only observed for 48 h (Figs. 2b, 3a, b). These results are an indicative that the peptide does not enter the parasite through transporters, which depend on the membrane potential, neither through receptor-mediated endocytosis nor fluid-phase pinocytosis at least to the studied period. Another possibility is that the low temperature is interfering with some unknown *L. amazonensis* cellular component that affects the interaction of $A_{36,42,44}Y_{32-46}$ *Vu*-Def. However, further studies should be

performed to better understand the mechanism behind *L. amazonensis* susceptibility to $A_{36,42,44}Y_{32-46}$ *Vu*-Def at 4 °C.

Conclusion

The results presented in the work indicate that the design and chemical synthesis of a 15 amino acid residues long peptide with amino acid substitutions based on the *Vu*-Defr plant defensin sequence, called $A_{36,42,44}Y_{32-46}$ *Vu*-Def, is biologically active and causes *L. amazonensis* culture inhibition by activation of an apoptotic-like cell death pathway. The results presented in this work reinforce the importance of the general strategy of amino acid substitution through mutagenesis or chemical synthesis which renders peptides with modified or improved biological activity to meet medical demand.

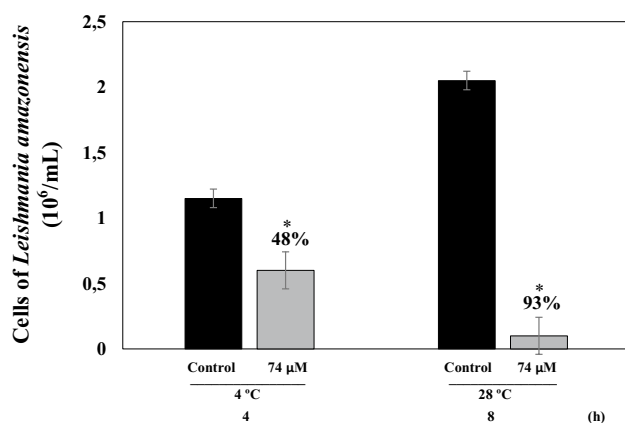


Fig. 8 Growth of *Leishmania amazonensis* promastigotes at 4 °C in the absence (control) and presence of 74 μM of the A_{36:42:44γ32:46}Vu-Def synthetic peptide. Growth was observed after 4 h incubation at 4 °C and after further 4 h at 28 °C. The percentage of protozoan inhibition is shown above the test bars. (*) Indicates significance ($p=0.0023$ for 4 °C; $p<0.0001$ for 28 °C) by the Tukey test ($p<0.05$) among the experiments and their controls. The graphic was done with the mean and standard deviation of one independent assay

Acknowledgements We acknowledge Luiz Carlos Dutra de Souza and Valéria Miguelote Kokis for their technical support. This work has received financial support of the Brazilian agencies Conselho Nacional de Desenvolvimento Científico e Tecnológico (CNPq), Fundação de Amparo a Pesquisa do Estado do Rio de Janeiro (FAPERJ, process no. E-26/102.981/2012-Bolsa; process no. E-26/202.760/2018-Bolsa), and the support of Universidade Estadual do Norte Fluminense. This study was financed in part by the Coordenação de Aperfeiçoamento de Pessoal de Nível Superior-Brasil (CAPES)-Finance Code 001.

Author contributions GSS and LPC performed the experiments; FCVS prepared the modeling; AOC and OLTM participated in the peptide design; EJTM, VMG and AOC participated in the protozoan experimental design and data analysis; GSS and AOC contributed to the writing of the manuscript.

Compliance with ethical standards

Conflict of interest The authors declare that they have no competing financial interests.

Human and animal rights statement This article does not contain any studies with human participants or animals performed by any of the authors.

References

- Akbari M, Oryan A, Hatam G (2017) Application of nanotechnology in treatment of leishmaniasis: a review. *Acta Trop* 172:86–90. <https://doi.org/10.1016/j.actatropica.2017.04.029>
- Altschul SF, Gish W, Miller W, Myers EW, Lipman DJ (1990) Basic local alignment search tool. *J Mol Biol* 215:403–410. [https://doi.org/10.1016/S0022-2836\(05\)80360-2](https://doi.org/10.1016/S0022-2836(05)80360-2)
- Ashibara T, Baserga R (1979) Cell synchronization. *Methods Enzymol* 58:248–262. [https://doi.org/10.1016/S0076-6879\(79\)58141-5](https://doi.org/10.1016/S0076-6879(79)58141-5)
- Baskić D, Popović S, Ristić P, Arsenijević NN (2006) Analysis of cycloheximide-induced apoptosis in human leukocytes: fluorescence microscopy using annexin V/propidium iodide versus acridin orange/ethidium bromide. *Cell Biol Int* 30:924–932. <https://doi.org/10.1016/j.cellbi.2006.06.016>
- Bjellqvist B, Hughes GJ, Pasquali C, Paquet N, Ravier F, Sanchez JC, Frutiger S, Hochstrasser D (1993) The focusing positions of polypeptides in immobilized pH gradients can be predicted from their amino acid sequences. *Electrophoresis* 14:1023–1031. <https://doi.org/10.1002/elps.11501401163>
- Bjellqvist B, Basse B, Olsen E, Celis JE (1994) Reference points for comparisons of two-dimensional maps of proteins from different human cell types defined in a pH scale where isoelectric points correlate with polypeptide compositions. *Electrophoresis* 15:529–539. <https://doi.org/10.1002/elps.1150150171>
- Carvalho AO, Gomes VM (2011) Plant defensins and defensin-like peptides—biological activities and biotechnological applications. *Curr Pharm Des* 17:4270–4293. <https://doi.org/10.2174/138161211798999447>
- Carvalho LP, Melo EJT (2018) intracellular development of *Trypanosoma cruzi* in the presence of metals. *J Parasit Dis* 42:372. <https://doi.org/10.1007/s12639-018-1010-2>
- Carvalho CS, Melo EJ, Tenório RP, Góes AJ (2010) Anti-parasitic action and elimination of intracellular *Toxoplasma gondii* in the presence of novel thiosemicarbazone and its 4-thiazolidinone derivatives. *Braz J Med Biol Res* 43:139–149. <https://doi.org/10.1590/S0100-879X2009005000038>
- Cools TL, Struyfs C, Drijfhout JW, Kucharíková S, Romero CL, Van Dijck P, Ramada MHS, Bloch C, Cammue BPA, Thevissen K (2017) A linear 19-mer plant defensin-derived peptide acts synergistically with caspofungin against *Candida albicans* biofilms. *Front Microbiol* 8:2051. <https://doi.org/10.3389/fmicb.2017.02051>
- de Figueiredo RC, Soares MJ (2000) Low temperature blocks fluid-phase pinocytosis and receptor-mediated endocytosis in *Trypanosoma cruzi* epimastigotes. *Parasitol Res* 86:413–418
- de Samblanx GW, Goderis JJ, Thevissen K, Raemaekers R, Fant F, Borremans F, Acland DP, Osborn RW, Patel S, Broekaert WF (1997) Mutational analysis of a plant defensin from radish (*Raphanus sativus* L.) reveals two adjacent sites important for antifungal activity. *J Biol Chem* 272:1171–1179. <https://doi.org/10.1074/jbc.272.2.1171>
- Fant F, Vranken WF, Borremans FAM (1999) The three-dimensional solution structure of *Aesculus hippocastanum* antimicrobial protein I determined by ¹H nuclear magnetic resonance. *Proteins* 37:388–403. [https://doi.org/10.1002/\(SICI\)1097-0134\(199911\)37:3<3388::AID-PROT7%3e3.0.CO;2-F](https://doi.org/10.1002/(SICI)1097-0134(199911)37:3<3388::AID-PROT7%3e3.0.CO;2-F)
- Fardin JM, Carvalho LP, Nascimento VV, Melo EJT, Gomes VM, Machado OLT, Vieira-Silva FC, Carvalho AO (2016) Biochemical purification of proteins from *Bertholletia excelsa* seeds and their antileishmanial action in vitro. *World J Pharm Res* 5:233–300. <https://doi.org/10.20959/wjpr20167-6609>
- Fázio MA, Oliveira VX, Bulet P, Miranda MTM, Daffre S, Miranda A (2006) Structure-activity relationship studies of gomesin: importance of the disulfide bridges for conformation, bioactivities, and serum stability. *Biopolymers* 84:205–218. <https://doi.org/10.1002/bip.20396>
- Figueira TN, Oliveira FD, Almeida I, Mello ÉO, Gomes VM, Castanho MARB, Gaspar D (2017) Challenging metastatic breast cancer with the natural defensin PvD₁. *Nanoscale* 9:16887–16899. <https://doi.org/10.1039/C7NR05872A>
- Gasteiger E, Hoogland C, Gattiker A, Duvaud S, Wilkins MR, Appel RD, Bairoch A (2005) Protein identification and analysis tools on the ExPASy server. *The proteomics protocols handbook*. Humana Press, Totowa, pp 571–607. <https://doi.org/10.1385/1-59259-890-0:571>

- Hayes BME, Bleackley MR, Anderson MA, van der Weerden NL (2018) The plant defensin NaD1 enters the cytoplasm of *Candida albicans* via endocytosis. *J Fungi* 4:20. <https://doi.org/10.3390/jof4010020>
- Jha S, Chattoo BB (2010) Expression of a plant defensin in rice confers resistance to fungal phytopathogens. *Transgenic Res* 19:373–384. <https://doi.org/10.1007/s11248-009-9315-7>
- Johansson J, Gudmundsson GH, Rottenberg ME, Berndt KD, Agerberth B (1998) Conformation-dependent antibacterial activity of the naturally occurring human peptide LL-37. *J Biol Chem* 273:3718–3724. <https://doi.org/10.1074/jbc.273.6.3718>
- Laskowski RA (1993) PROCHECK: a program to check the stereochemical quality of protein structures. *J Appl Cryst* 26:283–291. <https://doi.org/10.1107/S0021889892009944>
- Lobo DS, Pereira IB, Fragel-Madeira L, Medeiros LN, Cabral LM, Faria J, Bellio M, Campos RC, Linden R, Kurtenbach E (2007) Antifungal *Pisum sativum* defensin 1 interacts with *Neurospora crassa* cyclin F related to the cell cycle. *Biochemistry* 46:987–996. <https://doi.org/10.1021/bi061441j>
- Mangoni ML, Saugar M, Dellisanti M, Barra D, Simmaco M, Rivas L, Andrea OS, Molecolari P (2005) Temporins, small antimicrobial peptides with leishmanicidal activity. *J Biol Chem* 280:984–990. <https://doi.org/10.1074/jbc.M410795200>
- McGwire BS, Kulkarni MM (2010) Interactions of antimicrobial peptides with *Leishmania* and trypanosomes and their functional role in host parasitism. *Exp Parasitol* 126:397–405. <https://doi.org/10.1016/j.exppara.2010.02.006>
- Mukherjee SB, Das M, Sudhandiran G, Shaha C (2002) Increase in cytosolic Ca^{2+} levels through the activation of non-selective cation channels induced by oxidative stress causes mitochondrial depolarization leading to apoptosis-like death in *Leishmania donovani* promastigotes. *J Biol Chem* 277:24717–24727. <https://doi.org/10.1074/jbc.M201961200>
- Neto RLM, Sousa LMA, Dias CS, Filho JMB, Oliveira MR, Figueiredo RC (2011) Morphological and physiological changes in *Leishmania* promastigotes induced by yangambin, a lignan obtained from *Ocotea duckei*. *Exp Parasitol* 127:215–221. <https://doi.org/10.1016/j.exppara.2010.07.020>
- Pace D (2014) Leishmaniasis. *J Infect* 69:S10–S18. <https://doi.org/10.1016/j.jinf.2014.07.016>
- Pelegri B, Perseghini R, Silva ON, Franco L, Maria F (2011) Antibacterial peptides from plants: what they are and how they probably work. *Biochem Res Int* 2011:250349. <https://doi.org/10.1155/2011/250349>
- Reece SE, Pollitt LC, Colegrave N, Gardner A (2011) The meaning of death: evolution and ecology of apoptosis in protozoan parasites. *PLoS Pathog* 7:e1002120. <https://doi.org/10.1371/journal.ppat.1002320>
- Rodrigues IA, Azevedo MMB, Chaves FCM, Alviano CS, Alviano DS, Vermelho AB (2014) *Arrabidaea chica* hexanic extract induces mitochondrion damage and peptidase inhibition on *Leishmania* spp. *Biomed Res Int* 2014:985171. <https://doi.org/10.1155/2014/985171>
- Romestand B, Molina F, Richard V, Roch P, Granier C (2003) Key role of the loop connecting the two beta strands of mussel defensin in its antimicrobial activity. *Eur J Biochem* 270:2805–2813. <https://doi.org/10.1046/j.1432-1033.2003.03657.x>
- Sagaram US, Pandurangi R, Kaur J, Smith TJ, Shah DM (2011) Structure-activity determinants in antifungal plant defensins MsDef1 and MtDef4 with different modes of action against *Fusarium graminearum*. *PLoS One* 6:e18550. <https://doi.org/10.1371/journal.pone.0018550>
- Šali A, Blundell T (1993) Comparative protein modelling by satisfaction of spatial restraints. *J Mol Biol* 234:779–815
- Santos IS, Carvalho AO, de Souza-Filho GA, do Nascimento VV, Machado OLT, Gomes VM (2010) Purification of a defensin isolated from *Vigna unguiculata* seeds, its functional expression in *Escherichia coli*, and assessment of its insect α -amylase inhibitory activity. *Protein Expr Purif* 71:8–15. <https://doi.org/10.1016/j.pep.2009.11.008>
- Sarkar P, Jana K, Sikdar SR (2017) Overexpression of biologically safe *Rorippa indica* defensin enhances aphid tolerance in *Brassica juncea*. *Planta* 246:1029–1044. <https://doi.org/10.1007/s00425-017-2750-4>
- Schaaper WMM, Posthuma GA, Meloen RH, Plasman HH, Sijsma L, van Amerongen A, Fant F, Borremans FAM, Thevissen K, Broekaert WF (2001) Synthetic peptides derived from the β_2 - β_3 loop of *Raphanus sativus* antifungal protein 2 that mimic the active site. *J Pept Res* 57:409–418. <https://doi.org/10.1034/j.1399-3011.2001.00842.x>
- Sels J, Mathys J, De Coninck BMA, Cammue BPA, De Bolle MFC (2008) Plant pathogenesis-related (PR) proteins: a focus on PR peptides. *Plant Physiol Biochem* 46:941–950. <https://doi.org/10.1016/j.plaphy.2008.06.011>
- Seo M-D, Won H-S, Kim J-H, Mishig-Ochir T, Lee B-J (2012) Antimicrobial peptides for therapeutic applications: a review. *Molecules* 17:12276–12286. <https://doi.org/10.3390/molecules171012276>
- Soares JR, Melo JET, da Cunha M, Fernandes KVS, Taveira GB, da Silva Pereira L, Pimenta S, Trindade FG, Regente M, Pinedo M, de la Canal L, Gomes VM, Carvalho AO (2017) Interaction between the plant ApDef1 defensin and *Saccharomyces cerevisiae* results in yeast death through a cell cycle- and caspase-dependent process occurring via uncontrolled oxidative stress. *Biochim Biophys Acta Gen Subj* 1861:3429–3443. <https://doi.org/10.1016/j.bbagen.2016.09.005>
- Song X, Zhang M, Zhou Z, Gong W (2011) Ultra-high resolution crystal structure of a dimeric defensin SPE10. *FEBS Lett* 585:300–306. <https://doi.org/10.1016/j.febslet.2010.12.039>
- Souza GS, Nascimento VV, Carvalho LP, Melo EJT, Fernandes KV, Machado OLT, Retamal CA, Gomes VM, Carvalho AO (2013) Activity of recombinant and natural defensins from *Vigna unguiculata* seeds against *Leishmania amazonensis*. *Exp Parasitol* 135:116–125. <https://doi.org/10.1016/j.exppara.2013.06.005>
- Souza GS, Carvalho LP, Melo EJT, Gomes VM, Carvalho AO (2018) The toxic effect of Vu-Defr, a defensin from *Vigna unguiculata* seeds, on *Leishmania amazonensis* is associated with reactive oxygen species production, mitochondria dysfunction, and plasma membrane perturbation. *Can J Microbiol* 64:455–464. <https://doi.org/10.1139/cjm-2018-0095>
- Tavares PM, Thevissen K, Cammue BPA, Franc IEJA, Barreto-Bergter E, Taborda CP, Marques AF, Rodrigues ML, Nimrichter L (2008) In vitro activity of the antifungal plant defensin RsAFP2 against *Candida* isolates and its in vivo efficacy in prophylactic murine models of candidiasis. *Antimicrob Agents Chemother* 52:4522–4525. <https://doi.org/10.1128/AAC.00448-08>
- Terras FR, Goderis IJ, Van Leuven F, Vanderleyden J, Cammue BP, Broekaert WF (1992) In vitro antifungal activity of a radish (*Raphanus sativus* L.) seed protein homologous to nonspecific lipid transfer proteins. *Plant Physiol* 100:1055–1058. <https://doi.org/10.1104/pp.100.2.1055>
- Thevissen K, Kristensen H, Thomma BPHJ, Cammue BPA, François EJA (2007) Therapeutic potential of antifungal plant and insect defensins. *Drug Discov Today* 12:21–22. <https://doi.org/10.1016/j.drudis.2007.07.016>
- Torrent M, Pulido D, Rivas L, Andreu D (2012) Antimicrobial peptide action on parasites. *Curr Drug Targets* 13:1138–1147. <https://doi.org/10.2174/138945012802002393>
- Uchôa HB, Jorge GE, Da Silveira NJF, Camera JC, Canduri F, De Azevedo WF (2004) Parmodel: a web server for automated comparative modeling of proteins. *Biochem Biophys Res Commun* 325:1481–1486. <https://doi.org/10.1016/j.bbrc.2004.10.192>

- van der Weerden NL, Marilyn AA (2013) Plant defensins: common fold, multiple functions. *Fungal Biol Rev* 26:121–131. <https://doi.org/10.1016/j.fbr.2012.08.004>
- Vieira MEB, Vasconcelos IM, Machado OLT, Gomes VM, Carvalho AO (2015) Isolation, characterization and mechanism of action of an antimicrobial peptide from *Lecythis pisonis* seeds with inhibitory activity against *Candida albicans*. *Acta Biochim Biophys Sin* 47:716–729. <https://doi.org/10.1093/abbs/gmv071>
- Yount NY, Yeaman MR (2004) Multidimensional signatures in antimicrobial peptides. *Proc Natl Acad Sci USA* 101:7363–7368. <https://doi.org/10.1073/pnas.0401567101>

Publisher's Note Springer Nature remains neutral with regard to jurisdictional claims in published maps and institutional affiliations.